Journal of Solid State Chemistry **168,** 358–366 (2002)
doi:10.1006/jssc.2002.9673

Variable Dimensionality and New Uranium Oxide Topologies in the Alkaline-Earth Metal Uranyl Selenites $AE[(UO_2)(SeO_3)_2]$ (AE=Ca, Ba) and $Sr[(UO_2)(SeO_3)_2] \cdot 2H_2O$

Philip M. Almond, Shane M. Peper, Eric Bakker, and Thomas E. Albrecht-Schmitt[1,2]

Department of Chemistry, 179 Chemistry Building, Auburn University, Auburn, Alabama 36849

Received March 22, 2002; in revised form May 10, 2002; accepted May 28, 2002

DEDICATED TO THE 23RD RARE-EARTH RESEARCH CONFERENCE

Three new alkaline-earth metal uranyl selenites, $Ca[(UO_2)(SeO_3)_2]$ (1), $Sr[(UO_2)(SeO_3)_2] \cdot 2H_2O$ (2), and $Ba[(UO_2)(SeO_3)_2]$ (3), have been prepared from the reactions of $CaCO_3$ and $Ca(OH)_2$, $SrCl_2$ and $Sr(OH)_2$, or $BaCl_2$ and $Ba(OH)_2$ with UO_3 and SeO_2 under mild hydrothermal conditions. Single-crystal X-ray diffraction experiments reveal that the structures of 1–3 differ in both connectivity and dimensionality even though all contain the same fundamental building unit, namely $[UO_2(SeO_3)_4]$. This polyhedron consists of a linear uranyl unit that is bound by one chelating and three bridging selenite anions creating a pentagonal bipyramidal environment around the U(VI) center. The crystal structure of 1 contains one-dimensional ribbons where the edges are terminated by monodentate selenite anions. The interior of the ribbons are constructed from edge-sharing pentagonal bipyramidal UO_7 units. The structure of 2 is also one-dimensional; however, here there are chains of edge-sharing pentagonal bipyramidal UO_7 dimers that are connected by bridging selenite anions. $Ba[(UO_2)(SeO_3)_2]$ (3) is two-dimensional, and the highly ruffled anionic sheets present in this structure are formed from both bridging and chelating/bridging selenite anions bound to uranyl moieties. The anionic substructures in 1–3 are separated by Ca^{2+}, Sr^{2+}, or Ba^{2+} cations. Crystallographic data (193 K, Mo$K\alpha$, $\lambda = 0.71073$): 1, triclinic, space group $P\bar{1}$, $a = 5.5502(6)$ Å, $b = 6.6415(7)$ Å, $c = 11.013(1)$ Å, $\alpha = 104.055(2)^\circ$, $\beta = 93.342(2)^\circ$, $\gamma = 110.589(2)^\circ$, $Z = 2$, $R(F) = 4.56\%$ for 100 parameters with 1530 reflections with $I > 2\sigma(I)$; 2, triclinic, space group $P\bar{1}$, $a = 7.0545(5)$ Å, $b = 7.4656(5)$ Å, $c = 10.0484(6)$ Å, $\alpha = 106.995(1)^\circ$, $\beta = 108.028(1)^\circ$, $\gamma = 98.875(1)^\circ$, $Z = 2$, $R(F) = 2.43\%$ for 128 parameters with 2187 reflections with $I > 2\sigma(I)$; 3, monoclinic, space group $P2_1/c$, $a = 7.3067(6)$ Å, $b = 8.1239(7)$ Å, $c = 13.651(1)$ Å, $\beta = 100.375(2)^\circ$, $Z = 4$, $R(F) = 4.31\%$ for 105 parameters with 1824 reflections with $I > 2\sigma(I)$. © 2002 Elsevier Science (USA)

INTRODUCTION

The family of U(VI) compounds with oxoanions of Se(IV) and I(V) is rapidly expanding owing to the recent use of hydrothermal synthetic conditions (1–11). While crystalline solids with hexavalent uranium and iodate are unknown in nature, compounds containing the selenite anion have been structurally characterized in the rare minerals derriksite, $Cu_4[(UO_2)(SeO_3)_2](OH)_6$ (12), demesmaekerite, $Pb_2Cu_5[(UO_2)(SeO_3)_3]_2(OH)_6(H_2O)_2$ (13), guilleminite, $Ba[(UO_2)_3(SeO_3)_2O_2](H_2O)_3$ (14), and marthozite, $Cu[(UO_2)_3(SeO_3)_2O_2](H_2O)_8$ (15). The calcium uranyl selenite, piretite, $Ca[(UO_2)_3(SeO_3)_2(OH)_4] \cdot 4H_2O$, is also reported to contain the selenite anion, but its single-crystal structure is unknown (16). In addition, there is a growing group of synthetic uranyl selenite compounds that have been structurally characterized; these include $UO_2(SeO_3)$ (17), $UO_2(HSeO_3)_2 \cdot H_2O$ (18), $[NH_4]_2[UO_2(SeO_3)_2] \cdot 0.5H_2O$ (19), $A[UO_2(HSeO_3)(SeO_3)]$ ($A = NH_4$ (20), K (4), Rb (4), Cs (4), Tl (4)), $Ag_2(UO_2)(SeO_3)_2$ (4), and $Pb(UO_2)(SeO_3)_2$ (4).

Alkali, alkaline-earth, ammonium, main group, and transition metal cations play key structure-directing roles in the assembly of anionic uranium oxide topologies. In the case of uranyl iodates, substantial changes were observed when alkaline-earth metal cations were substituted for alkali metals in the preparation of $A_2[(UO_2)_3(IO_3)_4O_2]$ ($A = K$ (9), Rb (7), Tl (7)) and $AE[(UO_2)_2(IO_3)_2O_2](H_2O)$ ($AE = Sr$ (7), Ba (9), Pb (7)). These alterations can be even more pronounced when the cations actually form covalent bonds with the oxo groups in the uranium oxide moiety. This is demonstrated by $Ag_4(UO_2)_4(IO_3)_2(IO_4)_2O_2$ (8), which contains the previously unknown tetraoxoiodate,

[1] To whom correspondence should be addressed. Fax: 334 844-6959. E-mail: albreth@auburn.edu.

[2] Tables of anisotropic displacement parameters and structure factors for **1–3** are available from the author upon request.

0022-4596/02 $35.00

IO_4^{3-}, anion, and by $Pb(UO_2)(SeO_3)_2$ (4), which is an unusual example of a polar solid containing the uranyl cation.

In the absence of the influence of countercations, the combination of uranyl moieties with polydentate C_{3v} anions, such as selenite and iodate, should still result in a plethora of new compounds. This can be ascribed to the structural versatility of U(VI) which displays coordination environments ranging from six-coordinate $[UO_2X_4]^{n-}$ square bipyramids to seven-coordinate $[UO_2X_5]^{n-}$ pentagonal bipyramids to eight-coordinate $[UO_2X_6]^{n-}$ hexagonal bipyramids (21–23). Furthermore, the selenite anions are known to bind uranium in several different manners. These binding modes include monodentate, bridging, triply bridging, and simultaneous chelating and bridging. Therefore, by varying the structure-directing cations, the systematics of hydrothermal uranium chemistry can be greatly expanded and structure–property correlations can be made.

In this article, we report on the syntheses, crystal chemistry, and fluorescence spectroscopy of three new alkaline-earth metal uranyl selenites, $Ca[(UO_2)(SeO_3)_2]$ (**1**), $Sr[(UO_2)(SeO_3)_2]\cdot 2H_2O$ (**2**), and $Ba[(UO_2)(SeO_3)_2]$ (**3**). While these compounds have similar compositions, and for that matter nearly identical fundamental building units, their extended structures are quite divergent.

EXPERIMENTAL

Syntheses

UO_3 (99.8%, Alfa-Aesar), SeO_2 (99.4%, Alfa-Aesar), $SrCl_2\cdot 6H_2O$ (99.0%, Alfa-Aesar), $Sr(OH)_2\cdot 8H_2O$ (99.999%, Alfa-Aesar), $BaCl_2\cdot 2H_2O$ (97.0%, Fisher), $Ba(OH)_2\cdot 8H_2O$ (99.7%, Fisher), $CaCO_3$ (99%, Alfa-Aesar), and $Ca(OH)_2$ (98%, Fisher) were used as received. Distilled and Millipore filtered water with a resistance of 18 MΩ was used in all reactions. All reactions were run in PTFE-lined 23-mL Parr 4749 autoclaves. While the UO_3 contains depleted U, standard precautions for handling radioactive materials should be followed. Old sources of depleted U should not be used, as the daughter elements of natural decay are highly radioactive and present serious health risks. SEM/EDX analyses were performed using a JEOL 840/Link Isis instrument. Typical EDX analyses are within 4% of ratios determined from single-crystal X-ray diffraction experiments. IR spectra were collected on a Nicolet 5PC FT-IR spectrometer from KBr pellets.

*$Ca[(UO_2)(SeO_3)_2]$ (**1**)*

UO_3 (351 mg, 1.23 mmol), SeO_2 (272 mg, 2.45 mmol), $CaCO_3$ (123 mg, 1.23 mmol), $Ca(OH)_2$ (5 mg, 0.67 mmol), and 1.5 mL of water were loaded in a 23-mL PTFE-lined autoclave. The autoclave was sealed and placed in a preheated furnace for 30 days at 180°C. The furnace was then cooled at 9°C/h to 23°C. The product consisted of a clear and colorless solution over transparent, bright yellow prisms. The crystals were washed with methanol and allowed to dry. Yield, 614 mg (89% based on U). EDX analysis for $Ca[(UO_2)(SeO_3)_2]$ provided a Ca:U:Se ratio of 1:1:2. IR (KBr, cm^{-1}): ν(U≡O, U–O, and Se=O) 910 (m, br), 858 (m), 838 (m), 821 (m, sh), 807 (s), 741 (s, sh), 730 (s, sh), 719 (s).

*$Sr[(UO_2)(SeO_3)_2]\cdot 2H_2O$ (**2**)*

UO_3 (276 mg, 0.966 mmol), SeO_2 (214 mg, 1.931 mmol), $SrCl_2\cdot 6H_2O$ (153 mg, 573 mmol), and $Sr(OH)_2\cdot 8H_2O$ (257 mg, 0.966 mmol) were loaded in a 23-mL PTFE-lined autoclave. Water (1.5 mL) was then added. The autoclave was sealed and placed in a preheated furnace for 3 days at 180°C. The box furnace was cooled at 9°C/h to 23°C. The product consisted of a clear and colorless solution over transparent yellow prisms of **2**. The mother liquor with pH of 3.02 was decanted from the crystals. The crystals were then washed with methanol and allowed to dry. Yield, 446 mg (71% yield based on U). EDX analysis for $Sr[(UO_2)(SeO_3)_2]\cdot 2H_2O$ provided a Sr:U:Se ratio of 1:1:2. IR(KBr, cm^{-1}): ν(U≡O, U–O, and Se=O) 897 (m), 860 (m, sh), 849 (m), 807 (s), 761 (m), 731 (w), 690 (w), 659 (s), 618 (w).

*$Ba[(UO_2)(SeO_3)_2]$ (**3**)*

UO_3 (265 mg, 0.927 mmol), SeO_2 (205 mg, 1.854 mmol), $BaCl_2\cdot 2H_2O$ (193 mg, 0.790 mmol), and $Ba(OH)_2\cdot 8H_2O$ (87.5 mg, 0.329 mmol) were loaded in a 23-mL PTFE-lined autoclave. Water (1.5 mL) was then added. The autoclave was sealed and placed in a preheated furnace for 3 days at 180°C. The box furnace was cooled at 9°C/h to 23°C. The product consisted of a clear solution over transparent yellow prisms of **3**, UO_2SeO_3, and $BaSeO_3$. The mother liquor with a pH of 0.75 was decanted from the crystals. The crystals were washed with methanol and allowed to dry. Crystals of **3** were manually separated from UO_2SeO_3 and $BaSeO_3$ to provide a yield of 133 mg (22% based on U). EDX analysis for $Ba[(UO_2)(SeO_3)_2]$ provided a Ba:U:Se ratio of 1:1:2. The crystals IR(KBr, cm^{-1}): ν(U≡O, U–O, and Se=O) 883 (s), 878 (s), 860 (s), 838 (m), 809 (m), 756 (s), 726 (s, sh), 716 (s).

Crystallographic Studies

Crystals of $Ca[(UO_2)(SeO_3)_2]$ (**1**), $Sr[(UO_2)(SeO_3)_2]\cdot 2H_2O$ (**2**), and $Ba[(UO_2)(SeO_3)_2]$ (**3**) were mounted on glass fibers and aligned on a Bruker SMART APEX CCD X-ray diffractometer. Intensity measurements were performed using graphite monochromated Mo$K\alpha$ radiation

TABLE 1
Crystallographic Data for $Ca[(UO_2)(SeO_3)_2]$ (1), $Sr[(UO_2)(SeO_3)_2]\cdot 2H_2O$ (2), and $Ba[(UO_2)(SeO_3)_2]$ (3)

Formula	$Ca[(UO_2)(SeO_3)_2]$ (**1**)	$Sr[(UO_2)(SeO_3)_2]\cdot 2H_2O$ (**2**)	$Ba[(UO_2)(SeO_3)_2]$ (**3**)
Formula mass	564.03	647.60	661.29
Space group	$P\bar{1}$(No. 2)	$P\bar{1}$ (No. 2)	$P2_1/c$ (No. 14)
a (Å)	5.5502(6)	7.0545(5)	7.3067(6)
b (Å)	6.6415(7)	7.4656(5)	8.1239(7)
c (Å)	11.013(1)	10.0484(6)	13.651(1)
α (°)	104.055(2)	106.995(1)	90
β (°)	93.342(2)	108.028(1)	100.375(2)
γ (°)	110.589(2)	98.875(1)	90
V (Å^3)	364.01(7)	463.50(5)	797.1(1)
Z	2	2	4
T(°C)	−80	−80	−80
λ(Å)	0.71073	0.71073	0.71073
Maximum 2θ (deg.)	56.62	56.54	56.60
Observed data $I > 2\sigma(I)$	1530	2187	1824
ρ_{calcd} (g cm^{-3})	5.146	4.611	5.511
μ (Mo$K\alpha$) (cm^{-1})	330.05	310.88	343.41
$R(F)$ for $F_o^2 > 2\sigma(F_o^2)^a$	0.0456	0.0243	0.0431
$R_w(F_o^2)^b$	0.1019	0.0692	0.0936

[a] $R(F) = \sum||F_o| - |F_c||/\sum|F_o|$.
[b] $R_w(F_o^2) = \left[\sum\left[w(F_o^2 - F_c^2)^2\right]/\sum wF_o^4\right]^{1/2}$.

from a sealed tube and a monocapillary collimator. SMART was used for preliminary determination of the cell constants and data collection control. For all compounds, the intensities of reflections of a sphere were collected by a combination of three sets of exposures (frames). Each set had a different ϕ angle for the crystal and each exposure covered a range of 0.3° in ω. A total of 1800 frames were collected with an exposure time per frame of 30 s for **2** and **3** and 2 min for **1**. The long exposure time for **1** was necessitated by the small size of the crystal.

For **1**–**3**, determination of integral intensities and global cell refinement were performed with the Bruker SAINT (v 6.02) software package using a narrow-frame integration algorithm. A semi-empirical absorption correction was applied based on the intensities of symmetry-related reflections measured at different angular settings using SADABS (24) for **1**–**3**. An analytical absorption correction was also used for **2**. The program suite SHELXTL (v 5.1) was used for space group determination (XPREP), structure solution (XS), and refinement (XL) (25). The final refinements included anisotropic displacement parameters for all atoms and a secondary extinction parameter. Some crystallographic details are listed in Table 1 for **1**–**3**; additional details can be found in the Supporting Information. Atomic coordinates and isotropic displacement parameters for **1**–**3** are given in Tables 2–4.

Fluorescence Spectroscopy

Fluorescence characterization of **1**, **2**, and **3** was performed as previously described (10, 26). In summary, single crystals were placed onto a glass microscope slide and interrogated using a Nikon Eclipse E400 microscope with an epifluorescence attachment. Light from a 100-W mercury arc lamp was passed through a filter cube consisting of an excitation filter (425–475 nm), a dichroic mirror (480 nm), and a long-pass emission filter (> 495 nm). Emission was collected by a Plan Fluor objective lens (10×, 0.30 N.A.) and transmitted into a Peltier-cooled spectrometer coupled to a CCD detector (Cohu). Data processing was done on a PC using PARISS Spectral Imaging Software v. 6.0. For each crystal, an average spectrum was generated from 240 individual spectral lines. The exposure times used for crystal excitation were 400 ms for **1** and 1000 ms for **2** and **3**, respectively.

TABLE 2
Atomic Coordinates and Equivalent Isotropic Displacement Parameters for $Ca[(UO_2)(SeO_3)_2]$ (1)

Atom	x	y	z	U_{eq}(Å^2)[a]
U(1)	0.1670(1)	0.2596(1)	0.1671(1)	0.007(1)
Se(1)	0.7377(2)	0.7045(2)	0.3516(1)	0.007(1)
Se(2)	0.3126(2)	−0.1884(2)	0.1274(1)	0.009(1)
Ca(1)	0.6688(5)	0.2496(4)	0.4402(2)	0.008(1)
O(1)	0.3322(17)	0.0231(14)	0.2560(8)	0.011(2)
O(2)	0.4429(16)	0.3475(14)	0.0931(8)	0.009(2)
O(3)	−0.1085(17)	0.1748(14)	0.2474(8)	0.009(2)
O(4)	0.6826(17)	0.9062(14)	0.4563(8)	0.010(2)
O(5)	0.9298(17)	0.6222(14)	0.4338(9)	0.012(2)
O(6)	0.4432(17)	0.4855(14)	0.3522(8)	0.011(2)
O(7)	0.1075(17)	−0.4158(14)	0.1618(8)	0.010(2)
O(8)	0.1095(18)	−0.1272(14)	0.0315(9)	0.014(2)

[a] U_{eq} is defined as one-third of the trace of the orthogonalized $\mathbf{U}_{ij}$ tensor.

TABLE 3
Atomic Coordinates and Equivalent Isotropic Displacement Parameters for $Sr[(UO_2)(SeO_3)_2] \cdot 2H_2O$ (2)

Atom	x	y	z	$U_{eq}(Å^2)^a$
U(1)	0.1798(1)	−0.3205(1)	0.4381(1)	0.009(1)
Sr(1)	0.1545(1)	0.2635(1)	0.0120(1)	0.011(1)
Se(1)	0.2527(1)	0.0957(1)	0.3424(1)	0.010(1)
Se(2)	−0.3251(1)	−0.4153(1)	0.2794(1)	0.011(1)
O(1)	0.2024(7)	−0.5222(6)	0.2983(5)	0.015(1)
O(2)	0.1502(7)	−0.1138(6)	0.5662(5)	0.016(1)
O(3)	0.3122(7)	−0.1226(6)	0.3366(5)	0.013(1)
O(4)	−0.1260(6)	−0.3081(6)	0.2410(5)	0.012(1)
O(5)	−0.1665(6)	−0.4967(6)	0.4038(5)	0.014(1)
O(6)	−0.4510(7)	−0.6154(6)	0.1275(5)	0.016(1)
O(7)	0.4907(7)	0.2465(7)	0.4002(5)	0.018(1)
O(8)	0.1509(6)	0.0468(6)	0.1586(5)	0.015(1)
O(9)	0.3270(9)	0.0109(8)	-0.1210(6)	0.029(1)
O(10)	0.2107(6)	0.6392(6)	0.0444(5)	0.014(1)

[a] U_{eq} is defined as one-third of the trace of the orthogonalized $\mathbf{U}_{ij}$ tensor.

RESULTS AND DISCUSSION

Syntheses

In contrast to the preparation of alkali metal, transition metal, and main group uranyl selenites where the reactions of UO_3 and SeO_2 with the appropriate chloride salt yields the desired products, these reactions fail to produce alkaline-earth metal uranyl selenites when $CaCl_2$, $SrCl_2 \cdot 6H_2O$, or $BaCl_2 \cdot 2H_2O$ are used as starting materials. There are actually two requirements that must be fulfilled to successfully prepare $Ca[(UO_2)(SeO_3)_2]$ (**1**), $Sr[(UO_2)(SeO_3)_2] \cdot 2H_2O$ (**2**), and $Ba[(UO_2)(SeO_3)_2]$ (**3**). First, the pH of the reactions must be increased over that used to prepare $A[UO_2(HSeO_3)(SeO_3)]$ ($A = NH_4$ (20), K (4), Rb (4), Cs (4), Tl (4)), $Ag_2(UO_2)(SeO_3)_2$ (4), and $Pb(UO_2)(SeO_3)_2$ (4). Second, the reaction duration must be substantially lengthened in order to isolate **1** as a pure phase. The first requisite was accomplished by substituting some of the molar quantity of $AECl_2 \cdot nH_2O$ (AE = Sr, Ba) with $AE(OH)_2 \cdot nH_2O$ for **2** and **3**, and by using $CaCO_3$ and $Ca(OH)_2$ as the sources of Ca^{2+} cations in the preparation of **1**. In fact, these reactions are still quite acidic because of the formation of selenous acid. The pH values range from 3.02 to 0.75.

While 3-day reaction durations are appropriate for the preparation of **2** and **3**, in the synthesis of **1**, only $UO_2(SeO_3)$ (17) is observed after 3 days. Therefore, we sequentially increased the reaction duration and discovered that it required 1 month to prepare **1** as a pure compound. Our observations suggest that $UO_2(SeO_3)$ forms and precipitates in these reactions, but then further reacts with ions present in solution to form **1**. The syntheses of both uranyl selenites and iodates are plagued by the formation of $UO_2(SeO_3)$ (4) and $UO_2(IO_3)_2(H_2O)$ (5, 7, 8–10). In some cases, these compounds represent the major reaction product. It may well be that these simple compounds can be converted to desired products by utilizing long reaction durations. While this proved to be true for **1**, it was not for **3**, and $UO_2(SeO_3)$ was still observed with increased reaction durations. In this reaction, however, $BaSeO_3$ also forms, which means that a portion of the Ba^{2+} cations are being removed from solution, and therefore the persistence of $UO_2(SeO_3)$ is not surprising.

TABLE 4
Atomic Coordinates and Equivalent Isotropic Displacement Parameters for $Ba[(UO_2)(SeO_3)_2]$ (3)

Atom	x	y	z	$U_{eq}(Å^2)^a$
U(1)	0.2281(1)	0.0579(1)	0.3211(1)	0.008(1)
Ba(1)	0.6421(1)	0.0516(1)	0.1648(1)	0.010(1)
Se(1)	0.2861(1)	−0.2088(1)	0.5649(1)	0.008(1)
Se(2)	0.1277(1)	−0.2801(1)	0.1209(1)	0.009(1)
O(1)	0.2710(13)	−0.1008(12)	0.4571(7)	0.027(2)
O(2)	0.3933(12)	−0.3768(10)	0.5353(7)	0.020(2)
O(3)	0.4549(10)	−0.1010(10)	0.6414(6)	0.011(2)
O(4)	0.0015(10)	0.1407(9)	0.1736(6)	0.011(2)
O(5)	0.0749(11)	0.4608(9)	0.1725(6)	0.012(2)
O(6)	0.3343(10)	0.2376(9)	0.1975(6)	0.011(2)
O(7)	0.2851(11)	−0.1180(9)	0.2527(6)	0.013(2)
O(8)	0.1854(11)	0.2440(10)	0.3850(6)	0.013(2)

[a] U_{eq} is defined as one-third of the trace of the orthogonalized $\mathbf{U}_{ij}$ tensor.

Structures

$Ca[(UO_2)(SeO_3)_2]$ (1)

The structure of **1** is built from one-dimensional $^1_\infty[(UO_2)(SeO_3)_2]^{2-}$ ribbons that propagate down the b-axis and are separated from one another by Ca^{2+} cations. These one-dimensional ribbons are depicted in Fig. 1, and a packing diagram is shown in Fig. 2. The ribbons contain pentagonal bipyramidal U(VI) which is bound by two-terminal oxo groups, forming the uranyl moiety, and by one chelating/bridging, one monodentate/terminal, and two solely bridging selenite anions. Therefore, the fundamental building unit in this compound is $[UO_2(SeO_3)_4]$. These polyhedra edge-share to create dimers that are joined by the selenite anions. The orientation of the dimers is approximately perpendicular to the direction of chain propagation. While this same building unit has been observed in $Pb(UO_2)(SeO_3)_2$ (4), the manner by which these units condense in **1** is unique. In other words, **1** has an unprecedented structure type both in uranyl selenite compounds and in uranium oxides in general. The Ca^{2+} cations in **1** form eight contacts with surrounding oxygen atoms. These interactions range in distance from 2.312(9) to 2.774(9) Å and create a geometry that is best described

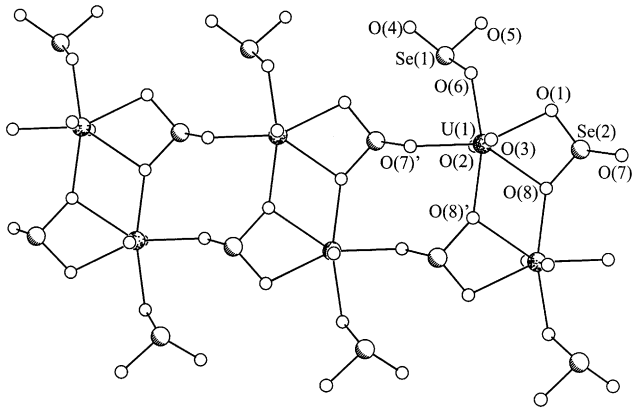

FIG. 1. A view of part of the structure of $Ca[(UO_2)(SeO_3)_2]$ (**1**) showing the one-dimensional $^1_\infty[(UO_2)(SeO_3)_2]^{2-}$ ribbons.

as a distorted dodecahedron. To date, this is the smallest cation that we have been able to incorporate between low-dimensional uranium oxide substructures by hydrothermal methods.

While there are only two crystallographically unique selenite anions, inversion operations allow this selenite anion, and symmetry-related selenite anions to occupy four of the five equatorial sites of the $[UO_7]$ pentagonal bipyramid. Two of the oxo groups in the equatorial plane are μ-O atoms and two are μ_3-O atoms. This actually creates substantial variations in the U–O distances, which range from 2.300(9) to 2.537(9) Å. In contrast, the U≡O bonds of the uranyl unit are 1.760(9) and 1.797(9) Å (see Table 5). The remaining selenite anion is monodentate and therefore has two terminal oxo groups that line the edges of the ribbons. Similar structural motifs have been observed in demesmaekerite, $Pb_2Cu_5[(UO_2)(SeO_3)_3]_2(OH)_6(H_2O)_2$ (13), and in uranyl idoates $A_2[(UO_2)_3(IO_3)_4O_2]$ (A = K (9), Rb (7), or Tl (7)) and $AE[(UO_2)_2(IO_3)_2O_2](H_2O)$ (AE = Sr (7), Ba (9), or Pb(7)).

TABLE 5
Selected Bond Distances (Å) for $Ca[(UO_2)(SeO_3)_2]$ (1)

U(1)–O(1)	2.434(8)	Se(1)=O(4)	1.672(8)
U(1)–O(2) (U≡O)	1.760(9)	Se(1)=O(5)	1.671(8)
U(1)–O(3) (U≡O)	1.797(9)	Se(1)=O(6)	1.767(9)
U(1)–O(6)	2.300(9)	Se(2)=O(1)	1.703(9)
U(1)–O(7)′	2.306(9)	Se(2)=O(7)	1.685(9)
U(1)–O(8)	2.537(9)	Se(2)=O(8)	1.715(9)
U(1)–O(8)′	2.374(9)		

The Se–O bonds are well within normal ranges, and there are correlations between these bond distances and the number of U–O(SeO_3) contacts that are formed. For instance, Se(1) has two Se–O terminal bond distances of 1.671(8) and 1.672(8) Å. However, the Se–O bond with the oxygen atom that coordinates the uranium center is lengthened to 1.767(9) Å. Likewise, of the three Se–O bonds to Se(2), the μ_3-O group has the longest Se–O bond of 1.715(9) Å, whereas the two μ-O atoms have Se–O distances of 1.703(9) and 1.685(9) Å.

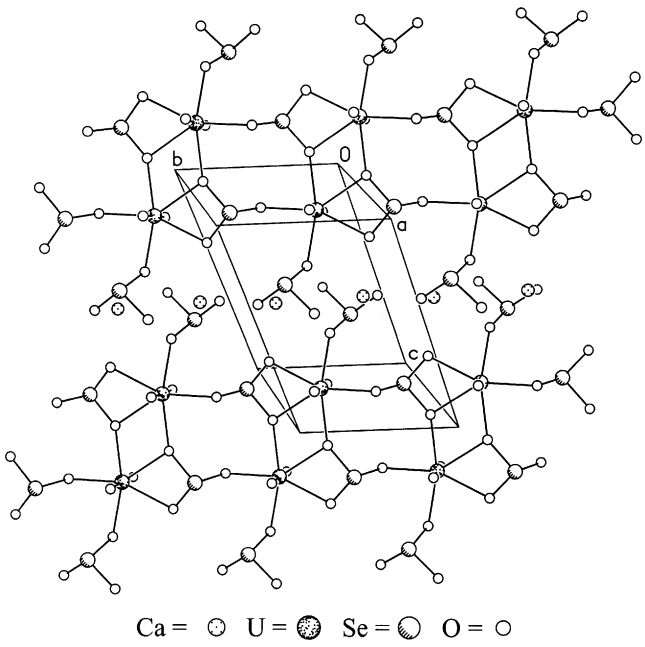

FIG. 2. A depiction of the packing of the one-dimensional $^1_\infty[(UO_2)(SeO_3)_2]^{2-}$ ribbons and Ca^{2+} cations in $Ca[(UO_2)(SeO_3)_2]$ (**1**).

$Sr[(UO_2)(SeO_3)_2]\cdot 2H_2O$ (**2**)

The structure of **2** is similar to that of **1** in that it consists of pentagonal bipyramidal $[UO_7]$ units that edge-share to create dimers that are in turn bridged together by selenite anions to create one-dimensional chains. We differentiate between the ribbons of **1** and the chains in **2** by the orientation of the uranium oxide dimers. In addition to other differences with **1** that will be discussed briefly, the dimers in **2** are oriented approximately parallel to the direction of chain propagation, as shown in Fig. 3. Again, we observe a similar $[UO_2(SeO_3)_4]$ fundamental building

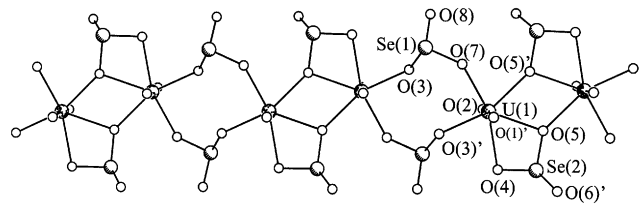

FIG. 3. An illustration of part of the structure of $Sr[(UO_2)(SeO_3)_2]\cdot 2H_2O$ (**2**) showing one-dimensional $^1_\infty[(UO_2)(SeO_3)_2]^{2-}$ chains where the dimers formed from edge-sharing $[UO_7]$ pentagonal bipyramids are oriented approximately parallel to the direction of chain propagation.

unit as found in **1**. However, here the five equatorial sites around the uranyl cation are occupied by one chelating/bridging and three bridging selenite anions. Therefore, the monodentate selenite anion found in **1** is absent in **2**.

The divergence between **1** and **2** also extends to the types of bridging selenite anions that are present. First, in **1** all bridging selenite anions are also chelating anions. Whereas in **2** one type of selenite anion simply bridges uranium centers and has one terminal oxygen atom. Second, in **1** all three oxygen atoms of the chelating selenite anion bind uranyl moieties, with the third oxygen atom acting to bridge uranium centers. In **2**, however, one of the oxygen atoms from the chelating selenite anion is terminal. In both **1** and **2**, the oxygen atoms that constitute the shared edge between the pentagonal bipyramids are μ_3-oxo groups. The structure type exhibited by **2** is most similar to those displayed by derriksite, $Cu_4[(UO_2)(SeO_3)_2](OH)_6$ (12), and $UO_2(HSeO_3)_2(H_2O)$ (18). In both of these compounds, there are one-dimensional chains consisting of uranyl polyhedra that are joined by bridging selenite anions. However, neither of these compounds contains edge-sharing dimers or chelating selenite anions.

While there is still considerable variation in the U–O bond lengths, particularly in the equatorial plane, the uranyl moiety itself is more symmetric in **2** than it is in **1**. Here the U≡O bond distances are 1.785(4) and 1.801(4) Å (see Table 6). This is probably because there are no short contacts between the uranyl cations and the Sr^{2+} cations, whereas in **1**, there is a 2.553(5) Å U≡O$\cdots$$Ca^{2+}$ interaction that creates asymmetry in the U≡O bond lengths. The five remaining U–O bonds in **2** range from 2.256(4) to 2.472(4) Å. The longest bonds are again to μ_3-O atoms. The Sr^{2+} cations form eight contacts with surrounding oxygen atoms to create a square antiprismatic environment. The $Sr^{2+}\cdots$O contacts range from 2.488(4) to 2.736(4) Å. The two water molecules in **2** are part of the coordination sphere of the Sr^{2+} cations and do not form close interactions with the one-dimensional chains. These water molecules form $Sr^{2+}\cdots O(H_2O)$ contacts of 2.659(5) and 2.678(4) Å. A diagram showing the separation of the one-dimensional chains by the Sr^{2+} cations and water molecules is depicted in Fig. 4.

TABLE 6
Selected Bond Distances (Å) for $Sr[(UO_2)(SeO_3)_2]\cdot 2H_2O$ (2)

U(1)–O(1) (U≡O)	1.801(4)	Se(1)=O(3)	1.733(4)
U(1)–O(2) (U≡O)	1.785(4)	Se(1)=O(7)	1.690(4)
U(1)–O(3)	2.268(4)	Se(1)=O(8)	1.663(4)
U(1)–O(4)	2.472(4)	Se(2)=O(4)	1.713(4)
U(1)–O(5)	2.458(4)	Se(2)=O(5)	1.724(4)
U(1)–O(5)′	2.390(4)	Se(2)=O(6)	1.664(4)
U(1)–O(7)′	2.256(4)		

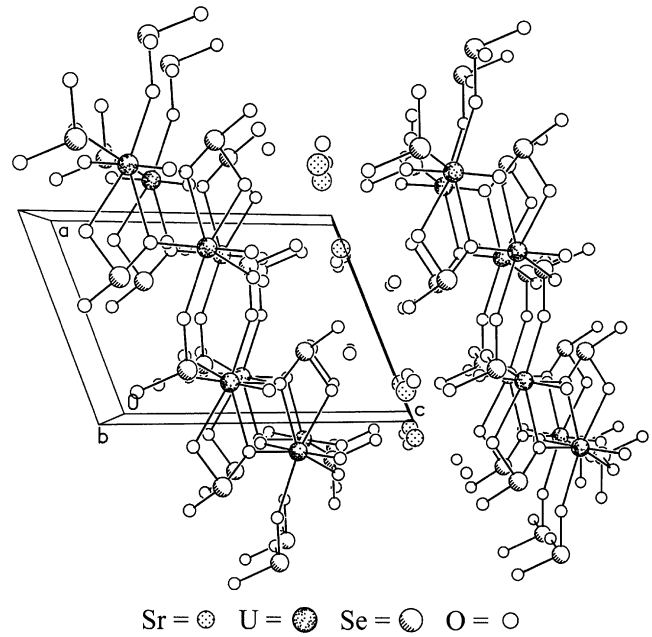

FIG. 4. A packing diagram of $Sr[(UO_2)(SeO_3)_2]\cdot 2H_2O$ (**2**) displaying the separation of the one-dimensional $^1_\infty[(UO_2)(SeO_3)_2]^{2-}$ chains by the Sr^{2+} cations and water molecules.

Ba[(UO$_2$)(SeO$_3$)$_2$] (3)

The structure of **3** is substantially different from that observed in **1** or **2** in that it consists of puckered two-dimensional $^2_\infty[(UO_2)(SeO_3)_2]^{2-}$ layers separated by Ba^{2+} cations. These layers are similar, but not identical, to those observed for $A[UO_2(HSeO_3)(SeO_3)]$ ($A = NH_4$ (18), K (4), Rb (4), Cs (4), Tl (4)), $Ag_2(UO_2)(SeO_3)_2$ (4), and $Pb(UO_2)(SeO_3)_2$ (4). The layers in **3** are shown in Fig. 5. This figure demonstrates that these layers are porous and that there is no condensation of uranyl polyhedra. In **3**, there are only long ionic contacts formed between oxygen atoms and the Ba^{2+} cations. There are nine $Ba^{2+}\cdots$O

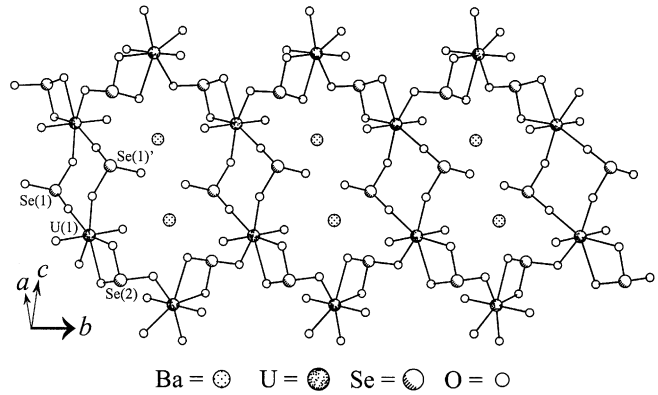

FIG. 5. A view of part of one of the $^2_\infty[(UO_2)(SeO_3)_2]^{2-}$ layers in $Ba[(UO_2)(SeO_3)_2]$ (**3**).

contacts ranging in distance from 2.699(8) to 3.155(8) Å that create a highly distorted tricapped trigonal prismatic environment around these cations. Part of the structure of **3** showing the $^{2}_{\infty}[(UO_2)(SeO_3)_2]^{2-}$ layers and the Ba^{2+} cations is depicted in Fig. 6. An unusual feature of this structure is that the Ba^{2+} cations do not actually lie between the layers rather they reside within the layers. This is the first time that we have observed this structural feature.

The same fundamental $[UO_2(SeO_3)_4]$ building unit is observed in **3** as is found in **1**, **2**, and $Pb(UO_2)(SeO_3)_2$. Oxygen atoms from bridging selenite anions occupy three of the five equatorial sites of the pentagonal bipyramid. One of these bridging selenite anions is also chelating an adjacent uranium center. Oxo groups from a chelating selenite anion fill the remaining two sites. The combination of the chelating/bridging and solely bridging selenite anions create fused and highly puckered rings containing six $[UO_2(SeO_3)_4]$ units. This compound represents yet another new uranyl selenite structure type that is most closely related to the anionic sheet topology (23) observed for $K_2[(UO_2)(MoO_4)_2]$ (27) where one of the vertices of the MoO_4^{2-} tetrahedra is removed to yield the trigonal pyramids of SeO_3^{2-}.

The U≡O bonds in **3** are the most symmetric of those observed for the compounds described herein, with bond distances of 1.797(8) and 1.800(8) Å (see Table 7). However, the O≡U≡O bond angle is the least linear of the three with angles of 178.2(4)°, 175.6(2)°, and 175.1(4)° being found for **1**, **2**, and **3**, respectively. Surprisingly, even though there are no μ_3-O atoms, the U–O bond distances in the equatorial plane vary from 2.236(9) to 2.459(8) Å.

Bond Valence Sums

The bond valence sums (BVSs) (28, 29) for the U(VI) centers in **1**–**3** were calculated using the parameters for seven-coordinate U(VI) given by Burns *et al.* (21). These calculations provide values of 5.95, 6.02, and 5.95 for the U(1) atoms in **1**, **2**, and **3**, respectively, and are therefore consistent with hexavalent uranium. The BVS of the Se(1) and Se(2) atoms in **1**, **2**, and **3** yield values ranging from 4.01 to 4.18, which are consistent with the presence of Se(IV).

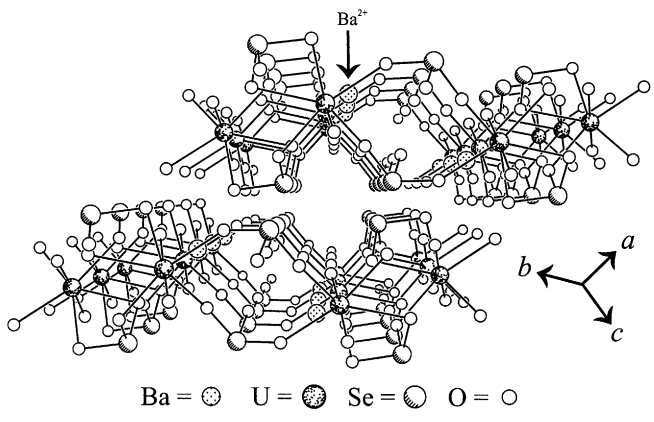

FIG. 6. An illustration of the packing of $Ba[(UO_2)(SeO_3)_2]$ (**3**) demonstrating that the Ba^{2+} cations are located within the porous $^{2}_{\infty}[(UO_2)(SeO_3)_2]^{2-}$ layers and do not separate these layers from one another.

TABLE 7
Selected Bond Distances (Å) for $Ba[(UO_2)(SeO_3)_2]$ (3)

U(1)–O(1)	2.236(9)	Se(1)=O(1)	1.699(9)
U(1)–O(3)′	2.307(7)	Se(1)=O(2)	1.660(8)
U(1)–O(4)	2.459(7)	Se(1)=O(3)	1.708(7)
U(1)–O(5)′	2.367(8)	Se(2)=O(4)	1.700(8)
U(1)–O(6)	2.459(8)	Se(2)=O(5)	1.702(7)
U(1)–O(7) (U≡O)	1.797(8)	Se(2)=O(6)	1.710(7)
U(1)–O(8) (U≡O)	1.800(8)		

Fluorescence Spectra

The emission of green light from uranyl-containing compounds when they are irradiated with UV light is a well-known phenomenon (30–32) and is commonly used to test for U(VI) in minerals. One of the characteristic features of this emission is the presence of the fine structure ascribed to the coupling of the excited state with U≡O vibrational modes, i.e., vibronic transitions. The electronic spectrum of $Cs_2UO_2Cl_4$ has been completely assigned by Denning and co-workers and can be used as a reference for other uranyl-containing compounds (32). However, it should be noted that not all uranyl-containing compounds fluoresce and the quantum yield from those that do varies dramatically. One of the mechanisms of non-radiative decay is vibrational coupling. For example, Grohol and Clearfield reported variances in the luminescent properties of two closely related uranyl phosphonates, $[UO_2(HO_3PC_6H_5)_2(H_2O)]_2 \cdot 8H_2O$ and $UO_2(HO_3PC_6H_5)_2(H_2O) \cdot 2H_2O$, whose structural differences are based largely on conformational differences in the phosphonates (33). In one case, emission was not observed until the sample was cooled to 77 K, indicating that vibrational coupling was likely responsible for non-radiative decay.

Compounds **1**–**3** represent an interesting case for study because they all contain the same $[UO_2(SeO_3)_4]$ fundamental building units, and should therefore display similar emission spectra. However, there may be two factors that mitigate the similarities of these spectra. First, the differences between the coordination modes of the selenite anions may have subtle influences on the electronic structure of these compounds. Second, close $AE^{2+}\cdots O(UO_2^{2+})$ interactions may provide a route for non-radiative decay. The spectra of **1**–**3** are depicted in Fig. 7. While these spectra are shown with an arbitrary intensity scale, the emission

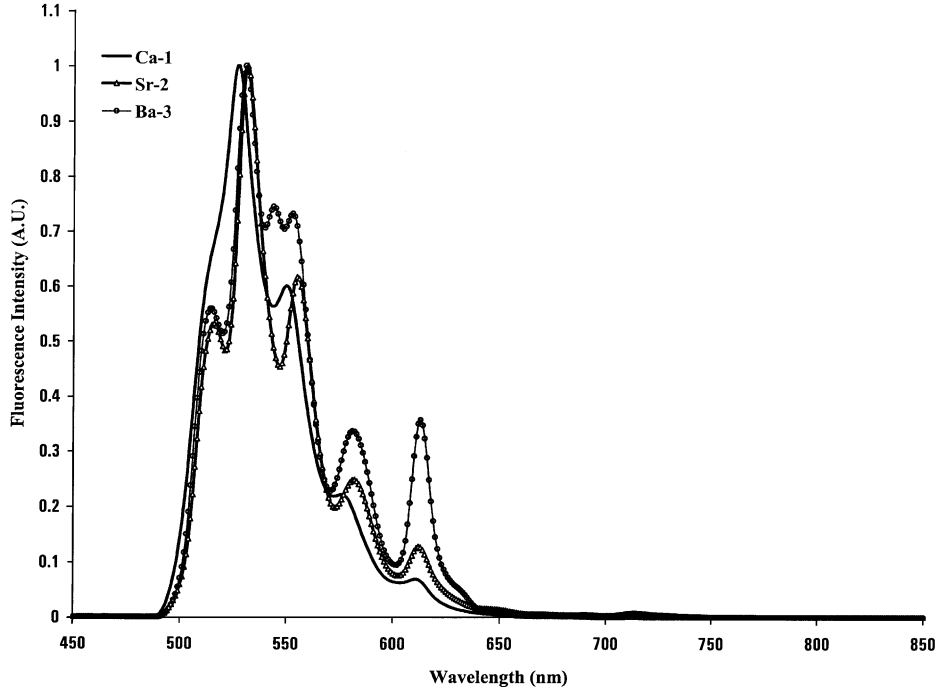

FIG. 7. Emission spectra of $Ca[(UO_2)(SeO_3)_2]$ (**1**), $Sr[(UO_2)(SeO_3)_2]\cdot 2H_2O$ (**2**), and $Ba[(UO_2)(SeO_3)_2]$ (**3**).

from **1** is much lower than that of **2** or **3**. Interestingly, of the three compounds reported herein, only **1** possesses close $AE^{2+}\cdots O(UO_2^{2+})$ interactions of 2.553(5) Å. Furthermore, the emission features from these compounds vary in width, location, and most importantly in the number of modes. As indicated by Fig. 7, **1** and **2** show five strong vibronic transitions, whereas **3** displays six. These spectra clearly indicate that non-covalent interactions and differences in the structures of **1**–**3** do affect the electronic properties of these compounds.

CONCLUSIONS

In the present study, we are finally starting to identify the structure-directing effects of countercations in the preparation of new uranyl selenite compounds. For all monocations used thus far, uranyl selenite layers similar to those found for $NH_4[UO_2(HSeO_3)(SeO_3)]$ (4, 20) are observed. This is true even when the countercation forms covalent bonds with the selenite anions as was found in $Ag_2(UO_2)(SeO_3)_2$ (4). When the cation becomes divalent, we find that the mode of ligation of the uranyl moiety changes from solely bridging selenite anions to a mix of chelating and bridging selenite anions, as was first observed in $Pb(UO_2)(SeO_3)_2$ (4). Therefore, there is a correlation between the fundamental building unit found with monovalent cations and that found with divalent cations. However, while all compounds with monovalent cations have similar uranyl selenite layers, all four uranyl selenites known with divalent cations have unique structure types.

ACKNOWLEDGMENT

Support for these studies was provided by the Department of Energy, Heavy Elements Program (Grant DE-FG02-01ER15187).

REFERENCES

1. A. Rabenau, *Angew. Chem. Int. Ed. Engl.* **24,** 1026 (1985).
2. J. W. Kolis and M. B. Korzenski, *in* "Chemical Synthesis Using Supercritical Fluids" (P. G. Jessop and W. Leitner, Eds.), Chap. 4. Wiley-VCH, New York, 1999.
3. A. K. Cheetham, G. Férey, and T. Loiseau, *Angew. Chem. Int. Ed. Engl.* **38,** 3268 (1999).
4. P. M. Almond and T. E. Albrecht-Schmitt, *Inorg. Chem.* **41,** 1177 (2002).
5. A. C. Bean, Y. Xu, J. A. Danis, T. E. Albrecht-Schmitt, and W. Runde, *Inorg. Chem.* submitted for publication (2002).
6. R. E. Sykora, D. M. Wells, and T. E. Albrecht-Schmitt, *Inorg. Chem.* **41,** 2304 (2002).
7. A. C. Bean and T. E. Albrecht-Schmitt, *J. Solid State Chem.* **161,** 416 (2001).
8. A. C. Bean, C. F. Campana, O. Kwon, and T. E. Albrecht-Schmitt, *J. Am. Chem. Soc.* **123,** 8806 (2001).
9. A. C. Bean, M. Ruf, and T. E. Albrecht-Schmitt, *Inorg. Chem.* **40,** 3959 (2001).
10. A. C. Bean, S. M. Peper, and T. E. Albrecht-Schmitt, *Chem. Mater.* **13,** 1266 (2001).

11. S. V. Krivovichev and P. C. Burns, *Can. Miner.* **39,** 207 (2001).
12. D. Ginderow and F. Cesbron, *Acta Crystallogr. C* **39,** 1605 (1983).
13. D. Ginderow and F. Cesbron, *Acta Crystallogr. C* **39,** 824 (1983).
14. M. A. Cooper and F. C. Hawthorne, *Can. Miner.* **33,** 1103 (1995).
15. M. A. Cooper and F. C. Hawthorne, *Can. Miner.* **39,** 797 (2001).
16. R. Vochten, N. Blaton, O. Peeters, and M. Deliens, *Can. Miner.* **34,** 1317 (1996).
17. B. O. Loopstra and N. P. Brandenburg, *Acta Crystallogr. B* **34,** 1335 (1978).
18. V. E. Mistryukov and Y. N. Michailov, *Koord. Khim.* **9,** 97 (1983).
19. M. Koshenlinna, I. Mutikainen, T. Leskelae, and M. Leskela, *Acta Chem. Scand.* **51,** 264 (1997).
20. M. Koshenlinna and J. Valkonen, *Acta Crystallogr. C* **52,** 1857 (1996).
21. P. C. Burns, R. C. Ewing, and F. C. Hawthorne, *Can. Miner.* **35,** 1551 (1997).
22. P. C. Burns, *in* "Uranium: Mineralogy, Geochemistry and the Environment" (P. C. Burns and R. Finch, Eds.), Chap. 1. Mineralogical Society of America, Washington, DC, 1999.
23. P. C. Burns, M. L. Miller, and R. C. Ewing, *Can. Miner.* **34,** 845 (1996).
24. SADABS, Program for absorption correction using SMART CCD based on the method of Blessing: R. H. Blessing. *Acta Crystallogr. A* **51,** 33 (1995).
25. G. M. Sheldrick, "SHELXTL PC, Version 5.0, An Integrated System for Solving, Refining, and Displaying Crystal Structures from Diffraction Data." Siemens Analytical X-ray Instruments, Inc., Madison, WI, 1994.
26. P. M. Almond, C. E. Talley, A. C. Gibbs, S. M. Peper, and T. E. Albrecht-Schmitt, *J. Solid State Chem.* **154,** 635 (2000).
27. G. G. Sadikov, T. I. Krasovskaya, Y. A. Polyakov, and V. P. Nikolaev, *Inorg. Mater.* **24,** 91 (1988).
28. I. D. Brown and D. Altermatt, *Acta Crystallogr. B* **41,** 244 (1985).
29. N. E. Brese and M. O'Keeffe, *Acta Crystallogr. B* **47,** 192 (1991).
30. F. Weigel, *in* "The Chemistry of the Actinide Elements" (J. J. Katz, G. T. Seaborg, and J. R. Morss, Eds.), Chap. 5. Chapman and Hall, London, 1986.
31. Carnall, W. T. and Crosswhite, H. M. *in* "The Chemistry of the Actinide Elements" (J. J. Katz, G. T. Seaborg, and J. R. Morss, Eds.), Chap. 16. Chapman and Hall, London, 1986.
32. Denning, R. G., Norris, J. O. W., Short, I. G., Snellgrove, T. R. and Woodwark, D. R., *in* "Lanthanide and Actinide Chemistry and Spectroscopy" (ACS Symp. Ser. no. 131), (N. M. Edelstein, Ed.), Chap. 15. American Chemical Society, Washington, DC, 1980.
33. D. Grohol and A. Clearfield, *J. Am. Chem. Soc.* **119,** 4662 (1997).